Anura3D
MPM Research Community

Comparison between Material Point Method and meshfree schemes derived from optimal transportation theory

Elizaveta Wobbes[1*], Roel Tielen[1], Matthias Moller[1], Cornelis Vuik[1], Vahid Galavi[2]

[1]Department of Applied Mathematics, Delft University of Technology, Delft, The Netherlands
[2]Geo-Engineering Section, Deltares, Boussinesqweg, 2629 HV Delft, Netherlands

* E-mail: e.d.wobbes@tudelft.nl

ABSTRACT

Both the Material Point Method (MPM) and meshfree schemes based on optimal transport theory have been developed for efficient and robust integration of the weak form equations originating from computational mechanics. Although the methods are derived in a different fashion, their algorithms share many similarities. In this paper, we outline the close resemblance of MPM and Optimal Transportation Meshfree (OTM) schemes. Aside from a theoretical analysis, the methods are compared numerically using a one-dimensional benchmark.

KEY WORDS: Material Point Method; Optimal Transportation Theory; Meshfree Methods.

INTRODUCTION

The Material Point Method (MPM) [Sulsky et al., 1994; Sulsky et. al., 1995] is a numerical technique suited to model large deformations in continuum mechanics. It originates from the fluid-dynamics-oriented Particle-In-Cell (PIC) method [Harlow,1964] and has been applied successfully in the numerical simulation of complex engineering problems [Sulsky et al., 2007; Zhang et al.,2008].
Optimal Transportation Meshfree (OTM) methods have been developed to simulate general solid and fluid flows and have been applied to a wide range of problems [Li et al., 2010; Fedeli et al., 2017; Navas et al., 2018]. OTM methods try to minimise the total action over a time interval, while using the conservation of mass as a constraint. Although MPM and OTM methods have different origin, many similarities can be found between them. In this paper, both methods are compared and analysed in detail. Since the methods have been developed and studied independently from each other, an in-depth comparison may lead to a further improvement of MPM based on the knowledge about the OTM method and vice versa. Numerical results obtained for a one-dimensional benchmark are presented before and after grid crossing occurs in MPM.
The paper is structured as follows: Both MPM and OTM are presented and each step of both algorithms is compared in Section 2. Numerical results obtained for one-dimensional benchmarks are presented in Section 3. Finally, conclusions are drawn in Section 4.

METHODS

The first part of this section provides OTM and MPM algorithms, whereas the second part outlines the similarities and explains the differences between them. The provided schemes are suitable for elastic solids and assume constant body forces.

Algorithms
The OTM scheme based on [Li et al., 2010] is presented in Algorithm 1, while the MPM algorithm [Sulsky et al., 1994] is shown in Algorithm 2. Algorithm 1 considers a general interpolation of the incremental transport map $\varphi_{k \to k+1}$:

$$\varphi_{h,k \to k+1}(x) = \sum_{a=1}^{N} x_{a,k+1} N_{a,k}(x), \tag{1}$$

where a indexes a nodal point, $\{N_{a,k}, a = 1, \ldots, N\}$ are the corresponding first-order consistent nodal basis functions at time t_k, and $\{x_{a,k}, a = 1, \ldots, N\} \equiv x_k$ is the array of nodal coordinates at time t_k. The shape functions are said to be consistent, when they satisfy the following conditions [Li et al., 2010]:

$$\sum_{a=1}^{N} N_{a,k}(x) = 1 \tag{2}$$

$$\sum_{a=1}^{N} x_{a,k} N_{a,k}(x) = x. \tag{3}$$

Algorithm 1 OTM

(1) Initialisation: Set k = 0, initialise nodal coordinates $x_{a,-1}$, $x_{a,0}$, material point coordinates $x_{p,-1}$, $x_{p,0}$, volumes $V_{p,0}$, densities $\rho_{p,0}$, masses m_p, stresses $\sigma_{p,0}$, and body forces b_p.

(2) Compute basis functions $N_{a,k}(x_{p,k})$ and derivatives $\nabla N_{a,k}(x_{p,k})$ from advected nodal and material-point sets.

(3) Determine the mass matrix M_k, linear momentum l_k, and force vector f_k:

$$M_{ab,k} = \sum_{p=1}^{M} m_p N_{a,k}(x_{p,k}) N_{b,k}(x_{p,k}), \tag{4}$$

$$l_{a,k} = \sum_{p=1}^{M} m_p \frac{x_{p,k} - x_{p,k-1}}{t_k - t_{k-1}} N_{a,k}(x_{p,k}), \tag{5}$$

$$f_{a,k} = \sum_{p=1}^{M} \left(\sigma_{p,k} \nabla N_{a,k}(x_{p,k}) + \rho_{p,k} b_p \right) V_{p,k}. \tag{6}$$

(4) Update the nodal coordinates:

$$x_{k+1} = x_k + (t_{k+1} - t_k) M_k^{-1} \left(l_k + \frac{t_{k+1} - t_{k-1}}{2} f_k \right). \tag{7}$$

(5) Update material point coordinates:

$$x_{p,k+1} = \varphi_{h,k \to k+1}(x_p, k). \tag{8}$$

(6) Update material point volumes:

$$V_{p,k+1} = det\left(\nabla \varphi_{h,k \to k+1}(x_{p,k}) \right) V_{p,k}. \tag{9}$$

(7) Update material point density:

$$\rho_{p,k+1} = \frac{m_p}{V_{p,k+1}}. \tag{10}$$

(8) Compute incremental strains at material point positions:

$$\Delta \varepsilon_{p,k+1} = \sum_{a=1}^{N} \nabla N_{a,k}(x_{p,k})(x_{a,k+1} - x_{a,k}). \tag{11}$$

(9) Update material point stresses using the constitutive equation:

$$\sigma_{p,k+1} \leftarrow \{\sigma_{p,k}, \Delta \varepsilon_{p,k+1}\}. \tag{12}$$

(10) Reset $k \leftarrow k + 1$. If $max(k)$ is reached, exit. Otherwise, go to (2).

Algorithm 2 illustrates the original MPM scheme that can cause numerical-stability issues when the number of empty elements changes during the computation [Sulsky et. al., 1995]. Therefore, this is not the most commonly used version of MPM, but can serve as a basis for the comparison with meshfree schemes derived from optimal transportation theory.

Algorithm 2 MPM

(1) Initialisation: Set k = 0, initialise nodal coordinates $x_{a,0}$, material point coordinates $x_{p,0}$, velocities $v_{p,0}$, volumes $V_{p,0}$, densities $\rho_{p,0}$, masses m_p, stresses $\sigma_{p,0}$, and body forces b_p.

(2) Compute basis functions $N_{a,0}(x_{p,k})$ and derivatives $\nabla N_{a,0}(x_{p,k})$ from advected material-point set.

(3) Determine the mass matrix M_k, linear momentum l_k, and force vector f_k:

$$M_{ab,k} = \sum_{p=1}^{M} m_p N_{a,0}(x_{p,k}) N_{b,0}(x_{p,k}), \tag{13}$$

$$l_{a,k} = \sum_{p=1}^{M} m_p v_{p,k} N_{a,0}(x_{p,k}), \tag{14}$$

$$f_{a,k} = \sum_{p=1}^{M} (\sigma_{p,k} \nabla N_{a,0}(x_{p,k}) + \rho_{p,k} b_p) V_{p,k}. \tag{15}$$

(4) Determine the nodal accelerations:

$$a_k = M_k^{-1} f_k. \tag{16}$$

(5) Update the nodal velocities:

$$v_k = M_k^{-1} l_k, \tag{17}$$

$$v_{k+1} = v_k + (t_{k+1} - t_k) a_k. \tag{18}$$

(6) Compute the incremental nodal displacement:

$$\Delta x_{k+1} = (t_{k+1} - t_k) v_{k+1}. \tag{19}$$

(7) Update material point coordinates:

$$x_{p,k+1} = x_{p,k} + \sum_{a=1}^{N} \Delta x_{a,k+1} N_{a,0}(x_{p,k}). \tag{20}$$

(8) Update the material point velocities:

$$v_{p,k+1} = v_{p,k} + (t_{k+1} - t_k) \sum_{a=1}^{N} a_{a,k+1} N_{a,0}(x_{p,k}). \tag{21}$$

(9) Update material point volumes:

$$V_{p,k+1} = det\left(\sum_{a=1}^{N} x_{a,k+1} \nabla N_{a,0}(x_{p,k})\right) V_{p,k}. \tag{22}$$

(10) Update material point density:

$$\rho_{p,k+1} = \frac{m_p}{V_{p,k+1}}. \tag{23}$$

(11) Compute incremental strains at material point positions:

$$\Delta\varepsilon_{p,k+1} = \sum_{a=1}^{N} \Delta x_{a,k+1} \nabla N_{a,0}(x_{p,k}). \tag{24}$$

(12) Update material point stresses using the constitutive equation:

$$\sigma_{p,k+1} \leftarrow \{\sigma_{p,k}, \Delta\varepsilon_{p,k+1}\}. \tag{25}$$

(13) Reset $k \leftarrow k + 1$. If $max(k)$ is reached, exit. Otherwise, go to (2).

_____

Comparison of the algorithms
Here, a side by side comparison of the computational steps from algorithm 1 and 2 is provided.
- In step 1, both algorithms intialise the nodal coordinates and material point properties.

- In step 2, the schemes compute the basis functions and their derivatives. However, in OTM basis functions are updated each time step based on the nodal velocities, while in MPM basis functions are fixed over time. This is an important difference between the methods. To distinguish between the basis functions, we denote OTM basis functions by $N_{a,k}$ and MPM basis functions by $N_{a,0}$.

- On the other hand, step 3 is identical for both schemes, because the material point velocity can be written as

$$v_{p,k} = \frac{x_{p,k} - x_{p,k-1}}{t_k - t_{k-1}}. \tag{26}$$

A direct substitution of Equation (26) into the expression for the linear momentum in the MPM algorithm (i.e. Equation (14)) leads to the linear momentum formula used in OTM, given by Equation (5).

- Furthermore, steps 4, 5, and 6 of Algorithm 2 are implicitly included in the computation of the nodal coordinates at time step $k + 1$ in Algorithm 1. To be more precise, from step 4 in the OTM scheme, we obtain

$$\Delta x_{k+1} = x_{k+1} - x_k = (t_{k+1} - t_k)M_k^{-1}\left(l_k + \frac{t_{k+1} - t_{k-1}}{2}f_k\right). \tag{27}$$

At the same time, the incremental nodal displacement in MPM can be written as

$$\Delta x_{k+1} = (t_{k+1} - t_k)v_{k+1} = (t_{k+1} - t_k)(v_k + (t_{k+1} - t_k)a_k) = (t_{k+1} - t_k)M_k^{-1}(l_k + (t_{k+1} - t_k)f_k). \tag{28}$$

Provided a constant time step, the above equation can be expressed as

$$\Delta x_{k+1} = (t_{k+1} - t_k)M_k^{-1}\left(l_k + \frac{t_{k+1} - t_{k-1}}{2}f_k\right). \tag{29}$$

From Equation (27) and (29) we conclude that, for constant time steps, MPM and OTM compute the nodal incremental displacement in the same manner.

- The definition of the incremental transport map implies that, in step 5 of Algorithm 1, material point positions are obtained from

$$x_{p,k+1} = \sum_{a=1}^{N} x_{a,k+1} N_{a,k}(x_{p,k}), \tag{30}$$

while step 7 in Algorithm 2 states that

$$x_{p,k+1} = x_{p,k} + \sum_{a=1}^{N} \Delta x_{a,k+1} N_{a,0}(x_{p,k}). \tag{31}$$

However, imposing Equation (3) on MPM, Equation (31) can be rewritten as follows

$$x_{p,k+1} = x_{p,k} + \sum_{a=1}^{N} \Delta x_{a,k+1} N_{a,0}(x_{p,k}) = \sum_{a=1}^{N} x_{a,k} N_{a,0}(x_{p,k}) + \sum_{a=1}^{N} \Delta x_{a,k+1} N_{a,0}(x_{p,k}). \tag{32}$$

Equation (32) can then be rewritten as

$$\sum_{a=1}^{N} x_{a,k} N_{a,0}(x_{p,k}) + \sum_{a=1}^{N} \Delta x_{a,k+1} N_{a,0}(x_{p,k}) = \sum_{a=1}^{N} x_{a,k+1} N_{a,0}(x_{p,k}). \tag{33}$$

- Moreover, the OTM scheme avoids a direct update of the material point velocity by adopting Equation (26), whereas MPM performs the update in step 8. Nevertheless, assuming that

$$v_{p,k} = \sum_{a=1}^{N} v_{a,k} N_{a,k}(x_{p,k}), \tag{34}$$

it is possible to relate the methods again. From the OTM algorithm, it follows that

$$v_{p,k+1} = \frac{x_{p,k+1} - x_{p,k}}{t_{k+1} - t_k}, \tag{35}$$

while substituting step 7 of Algorithm 2 leads to

$$v_{p,k+1} = \frac{x_{p,k+1} - x_{p,k}}{t_{k+1} - t_k} = \frac{\sum_{a=1}^{N} \Delta x_{a,k+1} N_{a,0}(x_{p,k})}{t_{k+1} - t_k} = \sum_{a=1}^{N} v_{a,k+1} N_{a,0}(x_{p,k}). \tag{36}$$

Steps 5 and 6 of Algorithm 2 imply that

$$v_{p,k+1} = \sum_{a=1}^{N} v_{a,k+1} N_{a,0}(x_{p,k}) = \sum_{a=1}^{N} v_{a,k} N_{a,0}(x_{p,k}) + \sum_{a=1}^{N} (t_{k+1} - t_k) a_{a,k} N_{a,0}(x_{p,k}) \qquad (37)$$

and, hence,

$$\sum_{a=1}^{N} v_{a,k} N_{a,0}(x_{p,k}) + \sum_{a=1}^{N} (t_{k+1} - t_k) a_{a,k} N_{a,0}(x_{p,k}) = v_{p,k} + (t_{k+1} - t_k) \sum_{a=1}^{N} a_{a,k} N_{a,0}(x_{p,k}). \qquad (38)$$

The final expression in Equation (38) is identical to the velocity update in step 8 in the MPM scheme. Although Equation (38) requires an extra assumption to establish a connection between the methods, it does not lead to an essential disparity between them.

- It is not difficult to see that the remaining part of the MPM algorithm is identical to that of the OTM.

In the above discussion, we have shown that under certain conditions the OTM and MPM schemes can be related. In fact, assuming a constant time step and the validity of Equation (3) and (34), the only difference between the methods emerges from the update of the basis functions.

NUMERICAL RESULTS

A one-dimensional linear-elastic vibrating bar is considered to assess the quality of both numerical schemes. The bar has fixed ends and its displacement is caused by an initial velocity, which is given by:

$$v(x,t) = 0.8 \sin\left(\frac{\pi x}{L}\right). \qquad (39)$$

Here, the length of the bar L equals 1 $[m]$, the Young's modulus E is $4 \cdot 10^4$ [Pa], and the density ρ is $2 \cdot 10^3 [\text{kg/m}^3]$. The domain is discretised using 20 elements and 8 material points per element. The time-step size is equal to 10^{-4} [s].
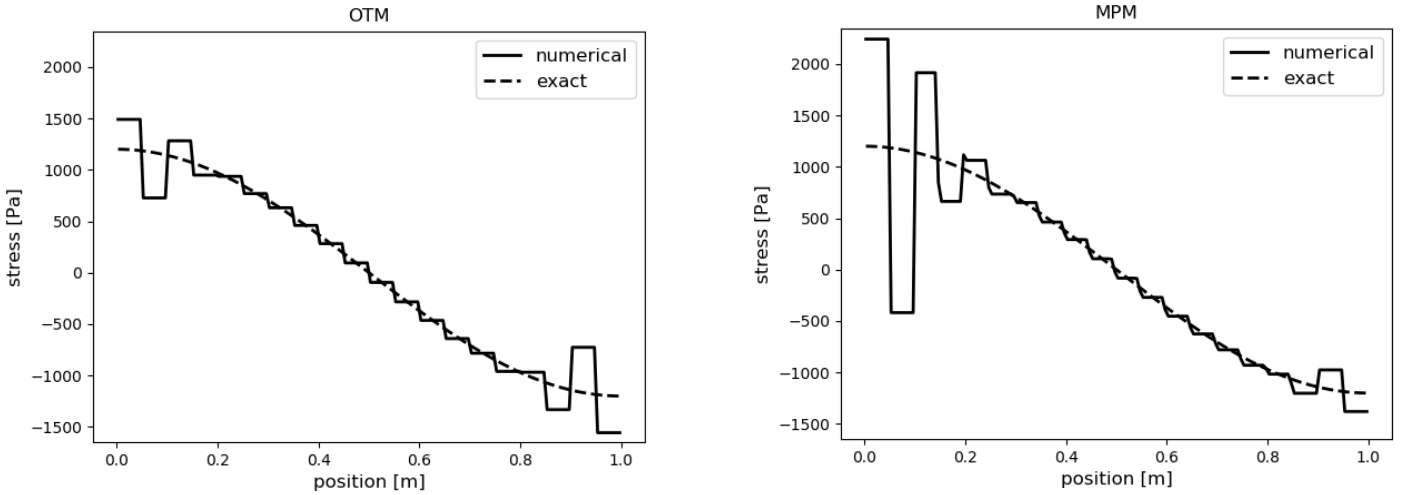

Figure 1 Comparison of numerical and analytical results in stress for OTM and MPM

Although typically OTM adopts meshfree maximum-entropy shape functions [Arroyo & Ortiz, 2006], the scheme can also be implemented with piecewise-linear (P1) basis functions commonly used in MPM. To focus on the comparison of the algorithms, in this paper, the computations are performed with P1 basis functions.

The analytical solution for the stress under small deformations is given by

$$\sigma(x,t) = 0.8\sqrt{E/\rho} \sin\left(\frac{\pi\sqrt{E/\rho}\,t}{L} \cos\left(\frac{\pi x}{L}\right)\right). \qquad (40)$$

In the beginning of the simulation, the results produced by MPM and OTM methods for this problem are very

similar. For example, after 20 times steps, the root-mean-square (RMS) error for the stress is equal to 3.8684 for OTM and 3.8693 for MPM. After material points start to move from one element to another in MPM, the solution quality of both schemes strongly decreases. However, the number of unphysical oscillations is higher for MPM and their amplitude in the neighbourhood of the left boundary is larger than that of the oscillations generated by OTM. This is illustrated in Figure 1.

CONCLUSIONS

In this paper, MPM has been compared to a meshfree scheme derived from optimal transportation theory (OTM). Assuming a constant time step size and Equation (3) and (34) to be valid, the only difference between the methods arises from the evaluation of the basis functions during the computation. To be more precise, within each time step, MPM computes the basis functions based only on the advected material-point set, whereas OTM also uses the advected nodal values. Numerical experiments performed on a one-dimensional linear-elastic vibrating bar have demonstrated that the application of MPM leads to a lower solution quality than OTM.

ACKNOWLEDGEMENTS

REFERENCES

Arroyo M & Ortiz M. (2006). Local maximum-entropy approximations schemes: a seamless bridge between finite elements and meshfree methods. *International Journal for Numerical Methods in Engineering*, 65(13): 2167-2202.
Fedeli L, Pandolfi A & Ortiz M. (2017). Geometrically exact time-integration mesh-free schemes for advection-diffusion problems derived from optimal transportation theory and their connection with particle methods. *International Journal for Numerical Methods in Engineering*, 112: 1175-1193.
Harlow F. (1964). The particle-in-cell computing method for fluid dynamics, *Methods for Computational Physics,* 3:319-343.
Li B, Habbal F & Ortiz M. (2010). Optimal transportation meshfree approximation schemes for fluid and plastic flows. *International Journal for Numerical Methods in Engineering*, 83: 1541-1579.
Navas, P., López‐Querol, S., Yu, R. C., & Pastor, M. (2018). Optimal Transportation Meshfree Method in Geotechnical engineering problems under large deformation regime. *International Journal for Numerical Methods in Engineering*.
Sulsky D, Chen Z & Schreyer H. (1995). Application of a particle-in-cell method to solid mechanics. *Computer Physics Communications*, 87:236-252.
Sulsky D, Schreyer H, Peterson K, Kwok R & Coon M. (2007). Using the material point method to model sea ice dynamics. *Journal of Geophysical Research*, 76:922-948.
Sulsky D, Zhou S & Schreyer H. (1994). A particle method for history-dependent materials. *Computer Methods in Applied Mathematics and Engineering*, 118:179-196.
Zhang D, Zou Q, VanderHeyden B & Ma X. (2008). Material point method applied to multiphase flows. *Journal of Computational Physics. 227:3159-3173.*